

Nonlinear effects in the torsional adjustment of interacting DNA

A. A. Kornyshev and A. Wynveen*

Department of Chemistry, Faculty of Physical Sciences, Imperial College, London SW7 2AZ, United Kingdom

(Received 10 November 2003; published 29 April 2004)

DNA molecules in solution, having negatively charged phosphates and counterions adsorbed on its surface, possess a distinct charge separation motif to interact electrostatically. If their double-helical structure were ideal, duplexes in parallel juxtaposition could choose azimuthal alignment providing attraction, or at least a reduction of repulsion, between them. But duplexes are not perfect staircases and the distortions of their helical structure correlate with their base pair texts. If the patterns of distortions on the opposing molecules are uncorrelated, the mismatch will accumulate as a random walk and attraction vanishes. Based on this idea, a model of recognition of homologous sequences has been proposed [A. A. Kornyshev and S. Leikin, *Phys. Rev. Lett.* **86**, 3666 (2001)]. But DNA has torsional elasticity. How will this help to relax a mismatch between the charge distributions on two nonhomologous DNA's? In the same work, the solution of this problem has been mapped onto a frustrated sine Gordon equation in a nonlocal random field (where the latter represents a pattern of twist angle distortions on the opposing molecules), but the results had been obtained in the limit of torsionally rigid molecules. In the present paper, by solving this equation numerically, we find a strongly nonlinear relaxation mechanism which utilizes static kink-soliton modes triggered by the "random field." In the range of parameters where the solitons do not emerge, we find good agreement with the results of a variational study [A. G. Cherstvy, A. A. Kornyshev, and S. Leikin, *J. Phys. Chem. B* (to be published)]. We reproduce the first-order transitions in the interaxial separation dependence, but detect also second-order or weak first-order transitions for shorter duplexes. The recognition energy between two nonhomologous DNA sequences is calculated as a function of interaxial separation and the length of juxtaposition. The soliton-caused kinky length dependence is discussed in connection with plots of recombination frequency as a function of the length of homology.

DOI: 10.1103/PhysRevE.69.041905

PACS number(s): 87.15.Aa, 87.15.Kg

I. INTRODUCTION

When two people meet in the forest they smile when approaching each other to do so without fear, unless external circumstances impel them to converge. Two lovers will adjust to each other to reach the closest embrace, whereas pugilists keep their fists up to prevent an embrace. Likewise peaceful relations between countries require friendly diplomatic overtures, which are not necessary in times of war, on the part of both parties.

The same rules apply to the world of macromolecules and colloids. If two objects that do not have a dominating attractive component in their interaction in their native state wish to approach each other, they need to "smile," i.e., to deform in a manner to become more attractive to each other. If they are driven toward each other by osmotic stress, they will be caused to "smile" to reach a lower energy state as they near each other.

The objects must be complementary when the attraction is already there without a "smile." This is a rare case which results in spontaneous irreversible aggregation. In contrast, a "smile" or a stronger reconstruction of noncomplementary objects is required to provide a crossover from repulsion to attraction. A "smile" alone may not warrant attraction, but "love at first sight"—a phenomenon in which there is a deep momentary phase-transition-like restructuring of the objects—does.

Three factors control these phenomena: (i) the intrinsic incommensurability of the interacting objects, (ii) the free energy gain in their mutually adjusted forms, and (iii) the free energy cost of the deformation needed, determined by the flexibility of the interacting objects. If the free energy gain prevails over the costs of deformation, attraction will emerge. Depending on the importance of the first factor, the attraction may grow smoothly, a "simile", or occur spontaneously, "love at first sight." In most of the cases these effects have a strong nonlinear character, and their description lies at the frontier of nonlinear science. In this paper we will explore them in the problem of interacting DNA.

A. DNA aggregation

DNA is a polyelectrolyte molecule. In solution it dissociates leaving negative charges on phosphates and positive counter charges either floating around the molecule or (partially) adsorbed onto its surface. It is, therefore, a common point that electrostatics should play an important role in DNA condensation, in the structure of DNA mesophases and morphology, and in the properties of dense aggregates [1,2]. It was not possible to rationalize many of these phenomena within the "primitive model" of a polyelectrolyte in which each DNA molecule was considered as a homogeneously charged cylinder [3]. The situation changed dramatically after it was shown that electrostatic interaction between DNA duplexes crucially depends on surface charge patterns [4].

Indeed, DNA in solution has a sophisticated charge distribution. The negative charges of phosphates follow the double helical symmetry of the molecule, whereas the adsorbed

*Electronic address: a.wynveen@imperial.ac.uk

cations reside in major/minor grooves or on the phosphate strings. Adsorption into the grooves causes distinct separation of positive and negative helical charge motifs along the molecule. Two such distributions on juxtaposing ideal helices will attract each other under a favorable mutual azimuthal alignment of the molecules [4]. This effect gives rise to the concept of the “electrostatic zipper motif for DNA aggregation” [5]. This attraction will take place even if the counterions are not localized in the grooves but are disordered on the surface. There still will be a charge separation motif due to the double helical pattern of the phosphates, but the attraction will be weaker in this case.

Aggregation does not mean the total collapse of the molecules because there is always a short-range repulsion [4]. This was found to be the “image” repulsion of the charge distribution on one molecule from the low dielectric constant core of the other molecule [this effect is represented in Eq. (1) of the present paper by $a_0(R)$]. For rigid ideal helices, this energy term as a function of R has twice as short of decay length as the attractive term [4], but it does not depend on the azimuthal orientations of the molecules. At even shorter distances there will be an additional hard-wall-like steric repulsion. If the charge on the phosphates is not fully compensated or is overcompensated by the readsorbed counterions, there may be double-layer-screened electrostatic repulsion at long distances. This will take place, however, only for sufficiently large net charges $>\approx 20\text{--}30\%$ of the charges on phosphates [4,5]. Below this, attraction will occur. Since attraction depends on the mutual azimuthal orientations of the molecules, DNA assemblies reveal a rich phase behavior [6–9].

B. DNA-DNA recognition

Basic equations describing this phenomenon were derived in Ref. [10], and it was argued that the attractive interaction may be responsible for a snap-shot electrostatic recognition of homologous DNA sequences at a distance. The first exploration of this hypothesis was based on the theory of the electrostatic interaction between DNA [4,5] which has been modified to include the sequence-dependent twist between adjacent base pairs [10]. It was found that the interaction between two DNA fragments of uncorrelated sequences differs dramatically from the interaction between two homologous sequences. Qualitatively, this result may be explained without complicated algebra, although a detailed theory allows quantifying the main effects [10].

Indeed, DNA is not a perfect staircase. Step angles are slightly distorted for each step, and the pattern of these distortions correlates with the text of the sequence [11,12]. Two rigid homologous duplexes in parallel juxtaposition will have almost identical patterns of distortions of the steps, and they can be aligned in such a way that the motifs of positive and negative charges will stay in register along the whole length of the sequence. This causes attraction between the sequences which locks them in close juxtaposition, necessary for the subsequent recombination process. On the contrary, two nonhomologous sequences have texts which are random with respect to each other. Their step distortions are unre-

lated. The quasihelical charge distributions on the juxtaposing duplexes can be positioned in register over a section of a certain length, but the register will be lost beyond this length for long enough duplexes. The attraction between them will therefore be much weaker or even turn into repulsion. This dramatic difference in the electrostatic interaction between homologous and nonhomologous DNA fragments allows the intact homologous sequences to recognize each other from a distance.

The characteristic length over which two juxtaposing torsionally rigid nonhomologous duplexes completely lose register, referred to as the helical coherence length, was found to be equal to $\lambda_c = h/\Delta\Omega^2$ [10], where h is the vertical rise between base pairs and $\Delta\Omega$ is the mean square fluctuation of the twist angle. For *B*-DNA $h \approx 3.4$ Å, $\Delta\Omega \approx 0.07\text{--}0.1$ rad [13–15] and thus $\lambda_c \approx 300\text{--}700$ Å. On length scales much larger than λ_c the torsional mismatch accumulates according to the law of a random walk. As it was shown in Ref. [10], rigid random duplexes longer than λ_c should always repel each other.

The always positive difference of the interaction between nonhomologous and between homologous duplexes of the same length was called “recognition energy.” It was found to be greater than $k_B T$ for sequences longer than 50 base pairs at DNA-DNA interaxial separations of $R = 30$ Å [10]. At closer interaxial separations the absolute value of the interaction energy increases nearly exponentially with diminishing R and so does the recognition energy. Two people recognize each other when they come closer, and the same applies on the macromolecular scale. The absolute value of the interaction energy, and consequently the recognition energy, is larger the longer the sequence.

This kind of electrostatic “snapshot” recognition mechanism may explain the enigmatic aspects of homologous recombination: (i) how genes responsible for the same function recognize each other and (ii) why the frequency of recombination events grows with DNA homology [16–21]. Shuffling of homologous genes takes place between father and mother DNA in sperm and oocytes before fertilization, or in the damaged genes replacement in DNA repair. It is a crucial element of evolution and genetic diversity. Recombination errors may lead to diseases such as cancer, Alzheimer’s, etc., and contribute to the aging process.

In order to understand the kinetics of homologous recombination, one must know what is the rate determining stage of it: the RecA-promoted recombination machinery in holiday junctions [22] or a precursor process of the recognition of homologous genes on the juxtaposing unzipped DNA [23,24]. Based on the former conjecture, a model with few fitting parameters has been proposed [25,26]. This model refers, however, to the fine tuning stage of recognition and not the coarse snapshot tuning from a distance. The latter is naturally explained by the electrostatic recognition of sequences as a whole [10]. This suggests a means for selective screening in a primary search [27] for homologous pairing in which DNA need not unzip. Note that the only earlier known recognition mechanism based on the base-pair complementarity of single strands [16] gives an opposite prediction: the recognition will be slower the longer the sequence. If the rec-

ognition is rate determining, this would translate into longer recombination times for longer sequences that have never been observed.

C. *In vitro* DNA aggregates

However, accepting this model we face a new problem. In most of the *in vitro* experiments DNA duplexes are not homologous. How come they are still able to spontaneously aggregate in the presence of DNA condensing counterions? A variational solution for this problem has been obtained in Ref. [28] that has incorporated torsional elasticity of the molecules.

Basic equations including torsional elasticity had been presented already in Ref. [10], but the detailed analysis had been presented under the assumption that the juxtaposing duplexes are torsionally rigid. There are experimental indications that DNA can torsionally relax as its structure changes in dense aggregates subject to external conditions. DNA overwinding from 10.5 base pairs per DNA helical pitch in solutions [29,30] to nearly 10 base pairs per pitch in hydrated fibers [31] as well as the *B*-to-*A* DNA transition at low humidity [32,33] have been recently explained by the gain in the corresponding electrostatic interaction energy of *ideal* duplexes [34,35].

D. Nonlinear phenomena

The main subject of the present article is the analysis of this problem over relevant length scales where the variational approach used in Ref. [28] is insufficient, i.e., to explore all the nonlinear aspects of the torsional adjustment. In formal terms, DNA has a finite torsional persistence length $\lambda_p = C/(k_B T)$, where C is the DNA torsional rigidity modulus. In addition, interacting DNA can be characterized by a torsional adaptation length λ_t [28], a quantity that reflects the combined effect of torsional elasticity and intermolecular interaction. Typical values of λ_t lie in the wide range of 20–700 Å [10]. For sequences longer than λ_t the effects of torsional elasticity cannot be ignored. The case of $2\lambda_c \geq \lambda_t$ has been analyzed in Ref. [28] whereas the case of $L \gg \lambda_t > \lambda_c$ is a primary suspect for more intricate nonlinear torsional behavior.

Torsional softness will help DNA aggregation but will, in turn, diminish the recognition energy. Will torsional flexibility completely wipe out the snapshot recognition mechanism? That was not the conclusion of Ref. [28] where the case of $2\lambda_c \geq \lambda_t$ has been considered. The recognition mechanism should certainly not be lost in the opposite case of rigid molecules. Our task is, therefore, to understand how the torsional softness relaxes nonhomology for any values L , λ_t , and λ_c .

Some of the new effects that we find below refer to molecules longer than λ_t that in turn is longer than λ_c . If we keep in mind that typical values of λ_c may be as large as 700 Å, we should be aware that for such long molecules other modes of relaxation could be available, primarily associated with DNA bending (whose persistence length is believed to be of the order of 500 Å) [36]. Our study is thus limited to an imposed constraint that parallel juxtaposition is somehow

provided. In fact we know almost nothing about the true structure of juxtaposition in the precursor stages of homologous recombination. But in columnar aggregates, stabilized by osmotic stress and/or condensed counterions, this complication may be neglected.

DNA torsional rigidity may greatly depend on external conditions, such as the adsorbed cations, solvent, temperature, etc. [37–39]. Thus, if the recognition energy is strongly influenced by finite torsional rigidity, there could be effects of external conditions on DNA-DNA recognition relevant to gene shuffling for genetic diversity and DNA repair.

II. PAIRWISE INTERACTIONS BETWEEN TWO DNA MOLECULES

The total Landau free energy of two parallel DNA molecules i and j in parallel juxtaposition consists of the electrostatic and the torsional energy terms, the latter associated with twist deformations of the individual helices about their preferred sequence-dependent twist angles $\Omega_i(z)$ and $\Omega_j(z)$. This energy was shown to be a functional of the relative local azimuthal orientation $\delta\phi(z) = \phi_i(z) - \phi_j(z)$, where z is the axial coordinate [10,28]

$$E \approx \int_0^L dz \left[a_0(R) - a_1(R) \cos[\delta\phi(z)] + a_2(R) \cos[2\delta\phi(z)] + \frac{C}{4} \left(\frac{d\delta\phi(z)}{dz} - \frac{\delta\Omega(z)}{h} \right)^2 \right]. \quad (1)$$

Here L is the length of the molecules, the a coefficients are electrostatic interaction parameters (for their detailed expressions, see Refs. [10,28]) that depend on the interaxial separation between the molecules R and the pattern of the charge distributions on them, and h is the helical rise per base pair (≈ 3.4 Å). The torsional term depends on the torsional elasticity modulus C and the difference in the preferential twist angles of the individual molecules at a given axial position $\delta\Omega(z) = \Omega_i - \Omega_j$. Again, the average twist angle for the *B*-DNA is $\langle \Omega \rangle = 34^\circ$ and the mean-squared sequence-dependent deviation from the average value is $\Delta\Omega = 4^\circ - 6^\circ$ [11–15].

Minimizing this energy yields the Euler-Lagrange equation for $\delta\phi(z)$ [10]

$$\frac{d^2[\delta\phi(z)]}{dz^2} - \frac{1}{\lambda_t^2} \sin[\delta\phi(z)] \left[1 - \frac{4a_2}{a_1} \cos[\delta\phi(z)] \right] = \frac{1}{h} \frac{d[\delta\Omega(z)]}{dz}. \quad (2)$$

The torsional length $\lambda_t = \sqrt{C/2a_1}$ depends on the ratio between the elasticity modulus and an interaxial-separation-dependent interaction constant. Both are sensitive to the environment and counterion adsorption patterns. Therefore λ_t depends on the solute, solvent, and temperature.

Note that the form of the energy functional and the resulting Euler equation with only one variable $\delta\phi(z)$ can be derived only when the torsional force constants are the same

for both molecules, otherwise we end up with two coupled nonlinear equations. Since we are going to consider interactions between different sequences, and we know that force constants can vary up to two times between different base pair dimers [15], we should consider the assumption of identical torsional constants as a simplifying one. For long sequences, however, the differences may average out.

This equation resembles that of a time-independent sine-Gordon equation, which appears in physical systems in different contexts: from Josephson junctions to nonlinear pendula (kicked rotator dynamics) [40]. The right-hand side (RHS) of the equation acts as an “external field” which has dramatic effects on the solutions for $\delta\phi(z)$, hereafter called the “phase angle.”

These solutions differ from those that may be found analytically for the homogeneous equation, i.e., when $\delta\Omega(z) = 0$. For infinitely long molecules the latter are drawn in Appendix A. They are of two types: z -independent solutions and kink-soliton solutions. The solitons are excitations in the system spectrum, as they have higher energies than z -independent solutions.

In an “external field” consisting of a few defects, effects of soliton pinning have been studied analytically in the pure sine-Gordon case [41]. This may result in energetically favorable kinklike solutions, or more precisely, solutions that utilize the soliton mode of response to an external perturbation. However, for a nonhomologous pair of DNA molecules, the random $\delta\Omega$ field is not simply a few defects, but rather a random field which is finite and varies over the entire axial length of juxtaposition.

As in the sine-Gordon equation with defects in the context of Josephson junctions [40] matters are complicated by the derivative of the “external field.” This means that $\delta\Omega$ acts nonlocally, as made more evident when rewriting Eq. (2) in terms of the random field integral $\Psi(z) = (1/h)\int_{z_0}^z dz' \delta\Omega(z')$ and the shifted phase angle

$$\begin{aligned} \widetilde{\delta\phi}(z) &= \delta\phi(z) - \Psi(z), \\ \frac{d^2[\widetilde{\delta\phi}(z)]}{dz^2} - \frac{1}{\lambda_l^2} \sin[\widetilde{\delta\phi}(z) + \Psi(z)] \\ &\times \left[1 - \frac{4a_2}{a_1} \cos[\widetilde{\delta\phi}(z) + \Psi(z)] \right] = 0. \end{aligned} \quad (3)$$

In order to go beyond the limiting cases that can be treated analytically, and also to consider strongly nonlinear effects, we solve Eq. (2) numerically and then calculate the corresponding ground-state energy of the system using Eq. (1).

III. THE APPROACH AND NUMERICAL PROCEDURE

For sine-Gordon equations of this type, global spectral or pseudospectral methods [42] which tend to be more accurate and efficient than local finite difference or finite element methods are ideally suited (see, e.g., Refs. [43,44]). However, instabilities may arise no matter what numerical techniques are used and are highly dependent on the parameters involved. Hence, convergence of correct solutions was only

assured after studies of the sensitivity of solutions to initial conditions, boundary conditions, and the range of the parameter space under scrutiny.

Employing standard spectral methods, the solutions to Eq. (2) are written as linear combinations of basis functions that possess simple derivative forms. The expansion coefficients are found by a rapidly converging procedure. Namely, these basis functions, evaluated at a series of collocation points (axial coordinates ideal for the basis functions being used), are substituted into a linearized form of the differential equation. This yields a set of residual equations in which the coefficients can be determined. Since the differential equation is nonlinear, this step is iterated via a Newton-Kantorovich scheme [42] until convergence of the expansion is achieved yielding an exact solution.

Solutions are considered unique (and exact) if identical solutions are obtained when using a different basis function expansion, employing expansions of different orders, or establishing boundary conditions by dissimilar means. To reflect the nonideality of the double helical staircase, the latter is modeled as steps each with a height of one helical rise ($\approx 3.4 \text{ \AA}$) but with a nonconstant twist angle that deviates from the average twist angle by approximately 0.1 radians [13–15]. At each rise, the difference of the preferred twist angles between two nonhomologous duplexes is modeled as a step with a Gaussian, randomly generated amplitude. The average value of these amplitudes is $\sqrt{\langle [\Omega_i(z) - \Omega_j(z)]^2 \rangle} = \sqrt{2\Delta\Omega^2}$. Obviously, such a way of incorporating helical nonideality is a strong simplification. Indeed, the vertical rise may fluctuate from step to step, and other angles, such as tilt and roll can also vary [11]. However, including these effects would entail exceeding the accuracy of the continuum model on which Eq. (2) rests.

Similar to the analytical explorations of this equation where results for the energy are found first for a given $\delta\Omega(z)$ and then are averaged over all its realizations, here, in each simulation, we solve the equation for the phase angle and calculate the energy for a specific form of $\delta\Omega(z)$. In the end, we may average the results to obtain an ensemble average of different realizations of $\delta\Omega(z)$, yielding a least square fit to the data with accompanying error bars.

Since the interaction is considered for finite-sized molecules, the boundary conditions must reflect the nature of the system. One can imagine three configurations: (i) the helices could be clamped at their ends, only allowed to wriggle about their middles; (ii) they could be clamped only at one end as if holding a snake by its tail with its head free to twist about; and finally, (iii) the entire length of the helices may be able to adjust their twist angles, subject to torsional constraints, to achieve the lowest total energy. Unless otherwise stated, the last configuration is considered as it yields the lowest energy state.

In reality, for extremely long chains, it is difficult to say how their extensions—beyond the region where the two macromolecules are within interaction distances and approximately parallel juxtaposition—influence the sections of the chains that are interacting. For numerical reasons, however, boundaries had to be maintained at the ends, to prevent instabilities and yield convergent solutions, and were ad-

justed to obtain the most energetically favorable state.

In this regard, we will hereafter neglect thermal fluctuations and only consider the lowest energy solutions. Thermal fluctuations may be quite important especially close to the second-order phase transition points seen in this model, but they will be treated elsewhere.

IV. COMPARISON OF NUMERICAL AND ASYMPTOTIC RESULTS

Since analytical expressions have been obtained for certain limiting cases of Eq. (2) [10,28], we began by testing the numerical simulations against the results of the analytical studies. We first summarize them.

For identical sequences, the RHS of Eq. (2) vanishes since the molecules share the same preferred twist angle pattern [$\delta\Omega(z) = \Omega_i(z) - \Omega_j(z) = 0$]. In the ground state the integrand of Eq. (1) does not depend on z , and the energy for this case, as shown in Fig. 1, has a single minimum above some interaxial separation, termed the “frustration point” [4], but two minima evolve below this point. This spontaneous broken symmetry for the energy leads to two separate solutions, which depend on the relative strengths of the electrostatic coefficients [4], for the optimal azimuthal angle between helices

$$\delta\phi_0 = \begin{cases} \pm \arccos(a_1/4a_2), & a_1 \leq 4a_2 \quad (R < R^*), \\ 0, & a_1 \geq 4a_2 \quad (R > R^*). \end{cases} \quad (4)$$

Here R^* , found from the condition that $a_1(R^*) = 4a_2(R^*)$, denotes the frustration point. The energy minima can then easily be found by substituting this optimal angle into Eq. (1)

$$E = \begin{cases} \left(a_0 - \frac{a_1^2}{8a_2} - a_2 \right) L, & R < R^*, \\ (a_0 - a_1 + a_2) L, & R > R^*. \end{cases} \quad (5)$$

For rigid molecules, or short chains, when $L \ll \lambda_c, \lambda_t$, the phase angle $\delta\phi(z)$ follows the accumulated random phase $\Psi(z)$. Substituting this into Eq. (1) and averaging over realizations of the Gaussian random field yields the interaction energy for rigid uncorrelated sequences obtained in Ref. [10]. For very rigid and/or short sequences this recognition energy was found to obey the rule [28]

$$\Delta E \approx a \frac{L^2}{2\lambda_c}, \quad (6)$$

where

$$a = \begin{cases} 4a_2 - a_1^2/4a_2, & R < R^*, \\ a_1 - 4a_2, & R > R^*. \end{cases} \quad (7)$$

If the duplexes are torsionally soft, i.e., $L, \lambda_c \gg \lambda_t$, they relax practically after every torsional mismatch, keeping the phase close to its optimal value. In this limit, then, the trigonometric functions in Eq. (2) can be expanded about $\delta\phi_0$ yielding an exactly solvable linear equation in $\delta\phi$ [28].

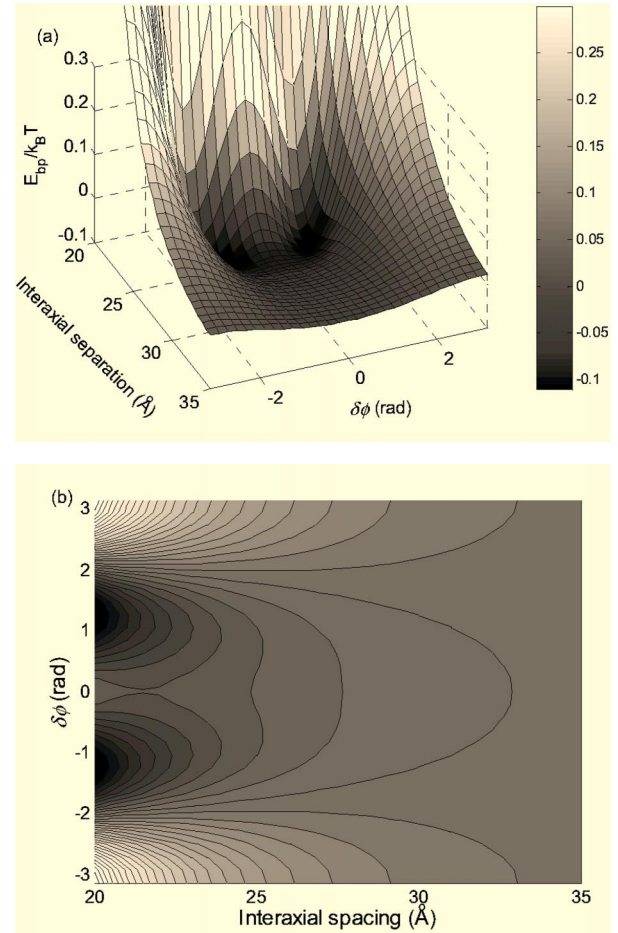


FIG. 1. The frustration of the electrostatic potential between DNA. The electrostatic interaction energy per base pair between identical DNA double helices in parallel juxtaposition is shown as a function of the relative azimuthal angle and their interaxial separation (a). At interaxial separations below $\approx 27 \text{ \AA}$ (for the chosen set of parameters) the energy possesses two degenerate minima, whereas there is only one minimum for larger separations. This is seen more easily in a contour plot of the energy (b) where the repulsive a_0 term is excluded from Eq. (1), i.e., only the terms dependent on azimuthal orientation are shown. (In both plots, darker shades represent lower energies.) The electrostatic coefficients, which vary with the interaxial separation, used for these plots are for helices with 90% counterion neutralization and a 30%/70% distribution of these ions between the minor and major grooves [10]. The same parameters are used in Figs. 7–10 of this paper.

Again, this solution can be substituted into Eq. (1) to find the energy, and hence, to find the corresponding recognition energy. In this case, it grows linearly with molecular length [28]

$$\Delta E \approx a \frac{\lambda_t}{2\lambda_c} L. \quad (8)$$

This makes perfect sense since the mismatch in the twist angles is not accumulated but relaxed at each step. Hence,

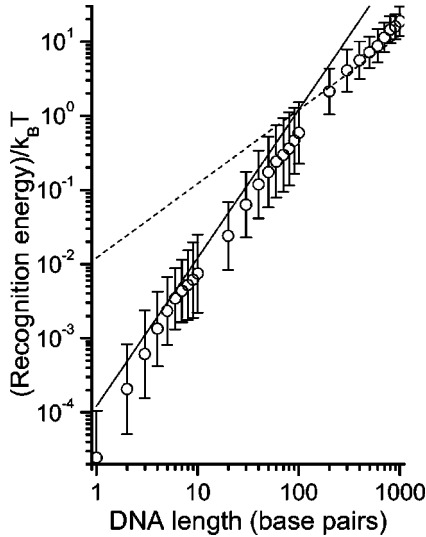


FIG. 2. Recognition energy as a function of DNA length averaged over 20 different simulations with their appropriate standard deviations. The solid line shows the quadratic relation for short molecules, Eq. (6), and the dashed line shows the linear relationship for long, flexible molecules, Eq. (8). For this set of numerical experiments $\lambda_t = \lambda_c$, where the coherence length is 100 base pairs. The electrostatic coefficients [5,10,28] for this plot are $a_0 = 1.2 \times 10^{-8}$ ergs/cm, $a_1 = 7.7 \times 10^{-8}$ ergs/cm, and $a_2 = 1.2 \times 10^{-8}$ ergs/cm. These values correspond to an interaxial separation between DNA of 30 Å.

the cost of torsional deformation energy yields an energy difference that is proportional to length.

To check if the numerical calculation of Eq. (2) subscribed to the analytic forms, (6) and (8), a series of different random field simulations were studied, yielding solutions for the phase angle. This was carried out first at interaxial separations above frustration $R > R^*$. (The effects of frustration are treated in a section to follow.) The difference in energy of this nonhomologous system, found from Eq. (1), and that of identical helices was then obtained to find the recognition energy. In this case, as with the analytical form (6), the helices were assumed to be fixed at one end at the angle optimal for identical helices. The random field fluctuation was defined as $\Delta\Omega = 0.1$ radians so that the coherence length was about 100 base pairs long.

The recognition energies obtained as the average of twenty different simulations are shown in Fig. 2. Again, only the lowest energy configurations were considered and were found via a global search over the “free” boundary, to eliminate any local minima, and then honing in on the lowest energy states. For shorter molecules, the recognition energy is approximately quadratic in length but becomes linear for increasingly longer molecules, exactly as advised by this theory.

V. NONLINEAR EFFECTS

Beyond the asymptotic laws, the numerical studies can check the variational results of Ref. [28] for $\lambda_t \leq \lambda_c$, where such nonlinear effects as a first order transition have been

found, and treat the regime $L \gg \lambda_t \gg \lambda_c$, where conditions are ripe for kink solitons. Here, the random walk accumulation yields large values of the phase angle which cannot relax in a linear fashion.

Although kink-soliton solutions are energetically less favorable when $\delta\Omega(z) = 0$ (Appendix A), incorporation of the random field admits the possibility that such solutions may yield lower energy configurations than those which simply follow the random field (torsionally rigid molecules) or those that simply relax the effects of $\delta\Omega$ at every step (torsionally soft molecules). In order to explore how solitonic effects may be turned on by a particular sequence, individual simulations with specific forms of $\delta\Omega$, mirroring experiments of interacting pairs with particular sequences, are also studied in addition to those averaged over different realizations of $\delta\Omega$.

A. Large fixed interaxial separations

We first investigate the effect of specific $\delta\Omega(z)$ profiles for a simpler case, when molecules are farther from each other than the frustration point R^* [of Eq. (4)]. The real experiments testing the length dependence of recombination generally have used segments of different lengths of a specific gene [17]. We simulate this by using longer and longer duplexes that incorporate the set of twist angles of the shorter ones. Namely, for a specific numerical simulation, a 400 base pair sequence will have the same form of the random field over its first 300 base pairs as that for the shorter 300 base pair sequence. Also, since the lowest energy solutions are desired, the boundary values of phase angle at either end are allowed to vary.

The phase angle profiles along with the recognition energy for a series of lengths, akin to that of Fig. 2, are diagrammed in Figs. 3–5 for a few random field generations. As evident in these figures, the recognition energy for specific profiles of the random field is no longer smooth.

At large interaxial separations, the optimal angle for minimization of the electrostatic interaction energy is $2n\pi$ (where $n = 0, \pm 1, \pm 2, \dots$). If there is enough accumulation of the mismatch in the preferential twist angle difference, the helices may find it energetically favorable to deform in such a way that the phase angle jumps from one electrostatic energy minimum to another. These effects will only be noticeable if the molecules are quite long since the width of a kink is approximately λ_t .

Figure 3(b) shows the phase angle for three different lengths. For the two shorter molecules, the random walk results in a kink forming near the right end of the molecule so that torsional energy is minimized. But as the molecule is made longer, this kink vanishes to minimize the electrostatic energy [45]. This is also apparent in the recognition energy, Fig. 3(a). It increases at the lengths at which this kink forms, but then levels off when the molecules are long enough to accommodate the kink.

Similar effects are also observed in Fig. 4. Here, shorter molecules have lowered their electrostatic energies by centering themselves about the optimal angle of zero

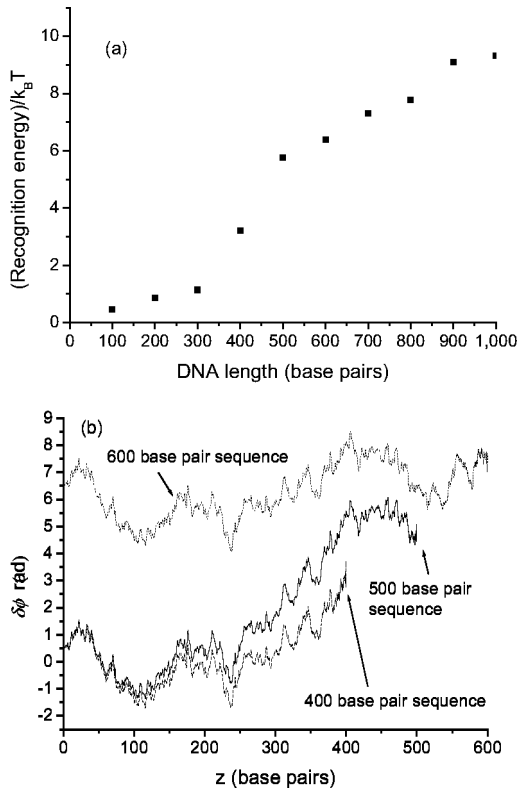


FIG. 3. The effect of a particular $\delta\Omega(z)$ set; the relaxed kinks. The recognition energy (a) is plotted as a function of molecular length with the corresponding phase angles shown for 400, 500, and 600 base pair long duplexes (b) for a particular twist angle distortion pattern. Here, relaxation of a kink is seen for longer molecules. In this simulation $\lambda_r = 5\lambda_c$. For these tests λ_c is artificially set at approximately 50 base pairs, although its natural value is considerably larger [10]. The values of the electrostatic coefficients are $a_0 = 5.8 \times 10^{-9}$ ergs/cm, $a_1 = 5.1 \times 10^{-9}$ ergs/cm, and $a_2 = 2.43 \times 10^{-10}$ ergs/cm, which corresponds to an interaxial distance of 35 Å and the counterion distribution given in Fig. 1.

degrees. But for longer molecules the interplay between electrostatic and torsional forces results in the phase angle sampling the zero and 2π electrostatic energy minima. Unlike the previous example, this change of the phase angle configuration is not as apparent in the recognition energy plot, Fig. 4(a). The increase of the recognition energy slightly diminishes when going from 400 to 500 base pairs as the kink turns on, which by no means could be inferred from a particularly “favorable” realization of the random field.

Figures 3(a) and 4(a) demonstrate similar behavior of the recognition energy although the phase angle patterns are different. This is due to the flexibility in these systems: in the case shown in Fig. 3 there is a gain in electrostatic energy and loss in torsional energy, whereas Fig. 4 corresponds to the opposite situation, yet the result is almost the same.

However, there are cases for specific forms of the random field in which the recognition energy displays a large deviation from a smoothly increasing curve that is not kink related as shown in Fig. 5. Here the recognition energy abruptly jumps and then levels off for molecules of lengths near 400 base pairs. This can be attributed to anomalously large

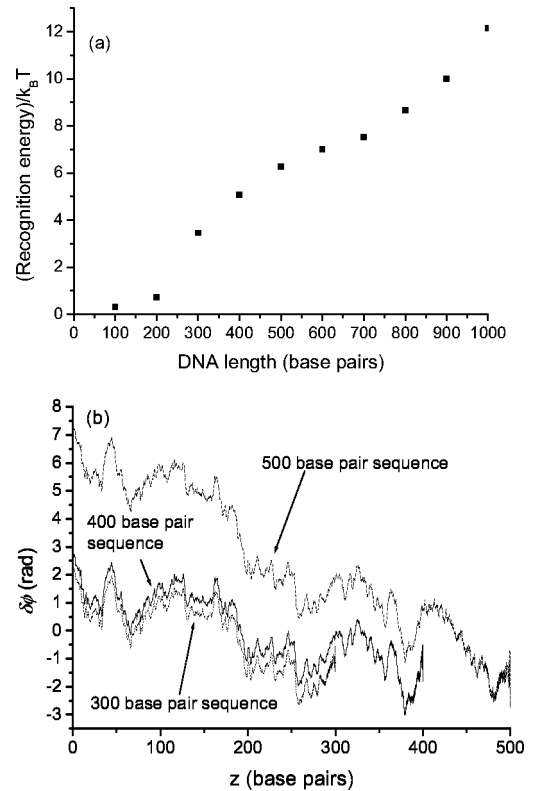


FIG. 4. Nonrelaxed kinks. The same is plotted here as in Fig. 3 for another simulation, i.e., another realization of $\delta\Omega$, for the same values of the electrostatic parameters. It shows that similar character of the recognition energy curve can be obtained for a different phase angle behavior. In this case, kink formation in the longer molecule is more energetically favorable for the system: the kink is not relaxed.

sequence-specific deviations in the random field. This is apparent in the solutions for the phase for this particular simulation shown in Fig. 5(b). This effect is not a prevailing factor in Figs. 3(b) and 4(b), where the offset of the phase angle plots for different lengths was unnecessary.

The above examples, nonetheless, illustrate that kink-like deformations of the molecules, which are inherent to Eq. (2), yield the most energetically favorable states.

Finally there is a special case of a nonrandom field, namely, $\delta\Omega(z) = \eta = \text{const}$, which is interesting from a physical point of view, because in this case the problem maps exactly on the Frenkel-Kontorova model [46]. Furthermore this case shows a linear accumulation of mismatch which is stronger than the average square-root accumulation for a Gaussian random walk. Biologically this is exotic if not irrelevant: this would be the case for $(AT)(AT)(AT)\cdots$ and $(GC)(GC)(GC)\cdots$ base pair sequences, although this could possibly be studied in special *in vitro* experiments. The results for this case are shown in Appendix B [47].

B. Varying the interaxial separation between molecules

The variational studies of Ref. [28] demonstrated novel effects as the molecules were approaching each other. Namely, a discontinuity in the optimal phase angle was dis-

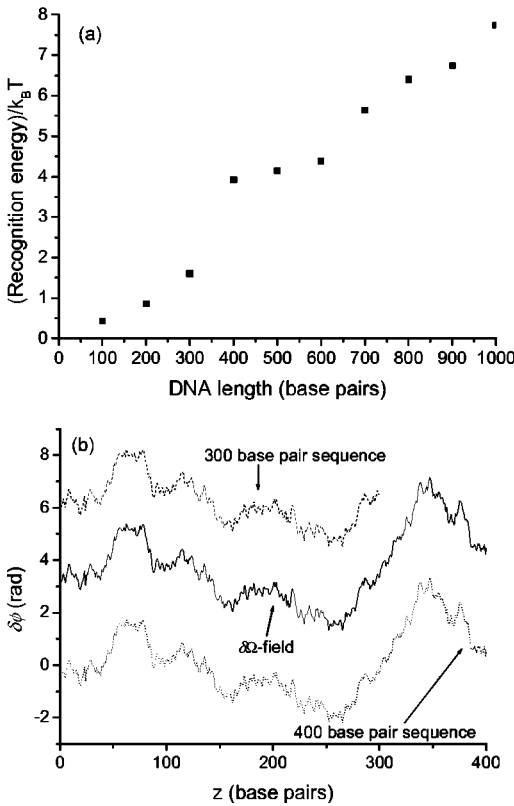


FIG. 5. “Response to a biased walk.” Again, the same is plotted here as in Figs. 3 and 4 but for a realization of $\delta\Omega$ which exhibits systematic deviations in one direction over a significant section of the juxtaposition length. The profile of $\delta\Omega$ is shown as the solid line in the phase angle graph. The large step in the recognition energy arises from anomalously large systematic deviations of the random field rather than due to the effect of kinks. This is seen going from a 300 base pair sequence (which is offset by 2π for clarification) to a 400 base pair sequence.

covered for interacting nonhomologous sequences below the frustration point. This first-order transition results from the removal of the spontaneous symmetry break of the optimal phase angle at the frustration point R^* . For identical helices this transition is second order, but this is no longer true when the random field is involved.

With decreasing interaxial distance between the molecules, the electrostatic forces begin to dominate the torsional forces, thus deforming the molecules. The electrostatic coefficients of Eq. (1) exponentially increase as the interaxial separation decreases. As the molecules approach each other, the effective torsional length λ_t decreases. Torsional deformations permit a better alignment of negatively charged strands and positively charged grooves of opposing molecules, reducing the electrostatic energy, but since they still cost energy, the electrostatic “mismatch” will never be totally relaxed. Therefore, the interaction energies for finite nonhomologous DNA are still greater than that of identical molecules, the recognition energy being larger for longer molecules.

Figure 6 shows the interaction energy as a function of interaxial separation for identical helices and an average for

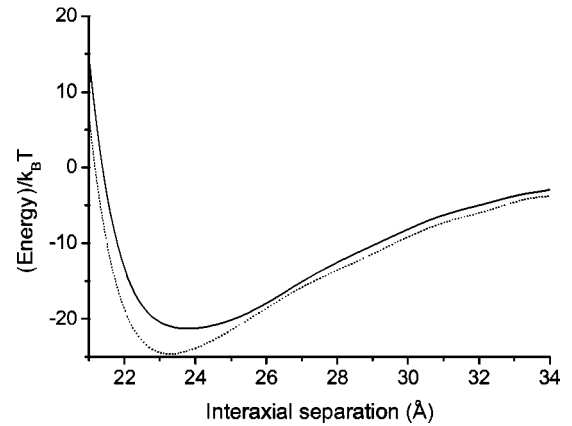


FIG. 6. Interaction energy: the effect of torsional relaxation. (T for dimensionless energy units is 300 K.) The curves are plotted for (dotted line) identical and (solid line) nonhomologous sequences with 210 base pairs using the same parameters as those used in Fig. 1 (see Ref. [28]). The nonhomologous curve is a least squares polynomial fit to five simulations with different $\delta\Omega$ profiles. The torsional constant $C = 3.0 \times 10^{-19}$ ergs cm here and for Figs. 7–10.

a set of nonhomologous sequences with different forms of the random field. The difference in the energies at their minima for the whole molecules will be greater than $k_B T$, and therefore, identical molecules can still be distinguished from nonhomologous molecules.

At separations below the frustration point, if the molecules are long enough or the random $\delta\Omega$ term tends to “walk” preferentially in one direction, both the electrostatic and torsional forces can be relaxed by a small kink between the $+/-$ optimal angles of Eq. (4). This is apparent in Fig. 7 where the phase angle at a separation above the transition jumps from one optimal angle to its negative. As the interaxial separation decreases, however, the electrostatic force dominates the torsional forces so that the phase angle only follows one of these optimal angles, also shown in Fig. 7.

This first-order transition is also apparent in the value of the phase angle averaged over the length of juxtaposition and in deviations about its mean value, Figs. 8(a) and 8(b). Below but close to the frustration point, the torsional forces are still relatively strong, and so it may be advantageous for the phase difference to sample both electrostatic energy minima at the $+/-$ optimal angles via a small kink. This results in a phase angle average near zero but with large fluctuations about this average.

If the molecules are pushed towards each other by an external force (osmotic stress), the electrostatic forces become stronger and the minima in the frustrated potential grows deeper. The small kinks then become energetically less favorable. Essentially, the helices “melt,” or are able to twist to the point where nearly perfect alignment about the optimal angle occurs. The deviations about the average therefore are reduced as seen in Fig. 8(b).

This first-order transition vanishes for shorter helices, however. Figures 9(a) and 9(b) show the mean value of the phase difference and fluctuations about this average, respectively, for molecules of different lengths. This makes perfect

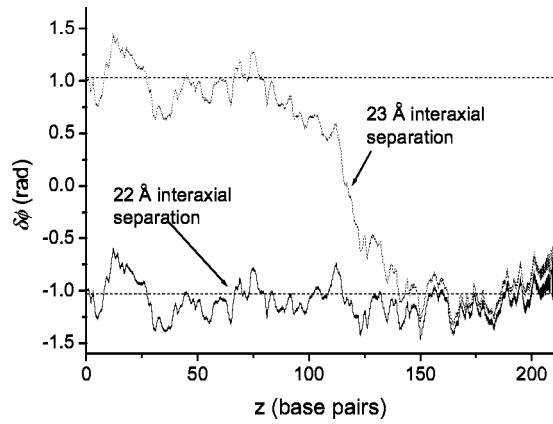


FIG. 7. Passing through a transition. The phase angle profiles of a sample simulation (specific random realization of $\delta\Omega$) showing what is happening when the interaxial separation passes through the transition. The solid line corresponds to a phase angle profile at an interaxial separation below the transition (≈ 22 – 23 Å). The dotted profile corresponds to a separation above the transition but still within the region of frustration, showing that the phase angle is shared via a kink between the two optimal angles. The horizontal dashed lines depict the optimal angles for identical helices, Eq. (4), below frustration at this same interaxial separation. This configuration reduces both the electrostatic energy and the torsional energy at this separation through the formation of a kink. A kink of this size would not likely be thermally activated in the absence of the random $\delta\Omega$ field: from Appendix A, its energy would be roughly $5k_B T$.

sense when one considers the accumulation of the random walk of $\delta\Omega$. For longer sequences, there will usually be enough accumulation to trigger a kink between the positive and negative optimal angles, as shown in Figs. 10(a) and 10(b). In contrast, for shorter sequences, there is not enough accumulation to favor a small kink, Fig. 10(c).

VI. DISCUSSION

In this work, we have explored regimes and described nonlinear effects which were beyond the reach of the analytical study [10,28] presented previously. Since the credibility of numerical solution of nonlinear equations with bifurcation options may always be questioned, comparisons between the numerical results and known solutions have been made. The numerical studies demonstrated consistency with the analytical, asymptotic results and approximate variational approach, which is a good sign. Together with many repeated simulations, began at different initial points, this suggests that we can trust the results in the “terra incognita” region that was inaccessible so far.

We have studied the energy of *recognition* of homologous and nonhomologous pairs of DNA duplexes. The recognition energy between torsionally flexible longer helices with finite rigidity increases linearly with length, but for shorter molecules, this recognition energy decreases faster. This form of the recognition energy suggests that longer helices can distinguish between identical helices and helices with different

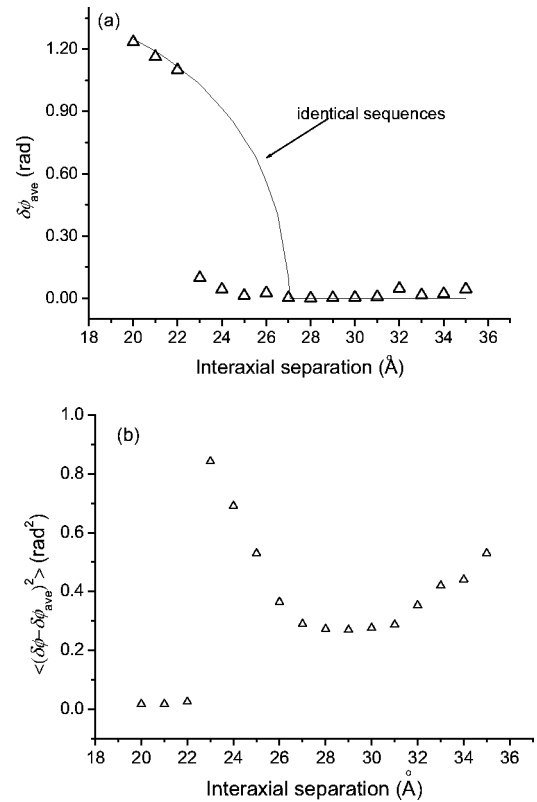


FIG. 8. First-order transition. The mean value of the phase angle over the length of the DNA (a) and the deviation about this average (b) are plotted as functions of the interaxial separation between two DNA. The solid line is for identical DNA, whereas the points correspond to a specific numerical simulation for nonhomologous sequences. As seen in these plots, a first-order transition is observed to occur somewhere between 22 and 23 Å for this particular simulation.

base pair sequences even when the helices are quite flexible. This corroborates the result of Ref. [28].

The numerical analysis also demonstrated that the most energetically favorable solutions may possess kink-like forms at large interaxial distances. These may manifest themselves in the recognition energies, but may not be discernable from consequences of the large fluctuations in the preferred twist angle differences. Such nonlinear effects are inherent to DNA [48–51], but this is the first treatment of those arising from DNA-DNA interactions before they unzip. It makes little sense to speculate about the possible “biological implications” of these soliton-like kinks, at the stage of computational explorations of their existence. Nevertheless, emergence of such torsional deformations is an interesting consequence of this model.

At interaxial separations below the point of frustration, smaller kinks between the positive and negative optimal angles (close to those that minimize the interaction energy of identical helices) may emerge. They are likely candidates to accompany homologous recombination. This possibility may in addition give rise to new interesting phenomena.

Indeed, variational studies [28] have revealed that there

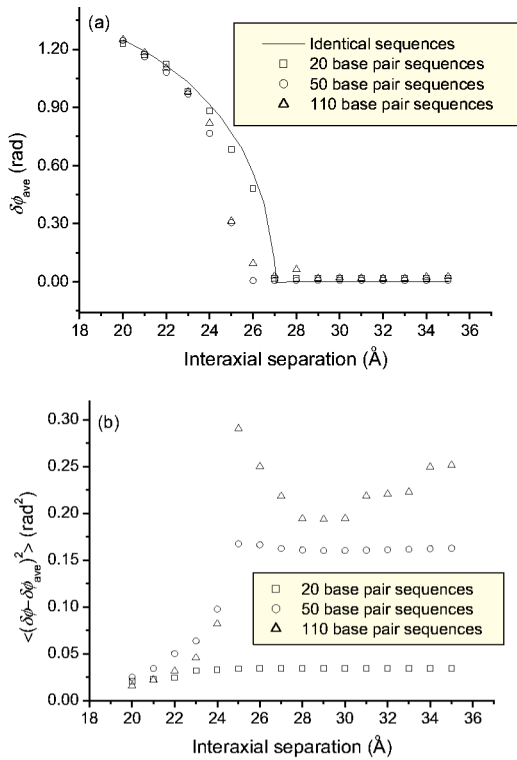


FIG. 9. Disappearance of first-order transition for short duplex pairs. The mean phase angle (a) and deviation from this average (b) are given for three different lengths. Note, the first-order transition is no longer seen for the shortest pair—there is not enough accumulation of the preferential twist angle difference nor is the molecule long enough to cause a small kink. This trend can be observed in Fig. 10 as well.

exists a first-order transition in the mean value of the phase angle when the duplexes approach each other. Numerical studies of this report (Figs. 8–10) have shown that small kinks easily form above this transition, but at the transition, the helices “snap” such that the kink is removed. Might this be expressed in homologous recombination? Certainly, claims of a direct correlation between the recombination frequency and the recognition energy curves should be taken with great care, if made at all. Nevertheless, it is curious that the switch from the first-order transition to second order occurs roughly at base pair lengths at which recombination frequencies drop abruptly, as seen in Fig. 11 which treats the data of Ref. [17]. Furthermore, for the set of parameters chosen for this exploration, the mentioned transition occurs at interaxial separations near the interaction energy minimum [Eq. (1)], a comfortable position for a recognition stage.

For shorter molecules on the order of the torsional length, there would be no “kink mechanism” to influence this stage. As observed in experiments (see Fig. 11) [17], extremely slow recombination, if any at all, occurs for shorter strands. The “minimal effective processing segment” [52] corresponds to strand lengths where we observe the switch between the two types of transitions.

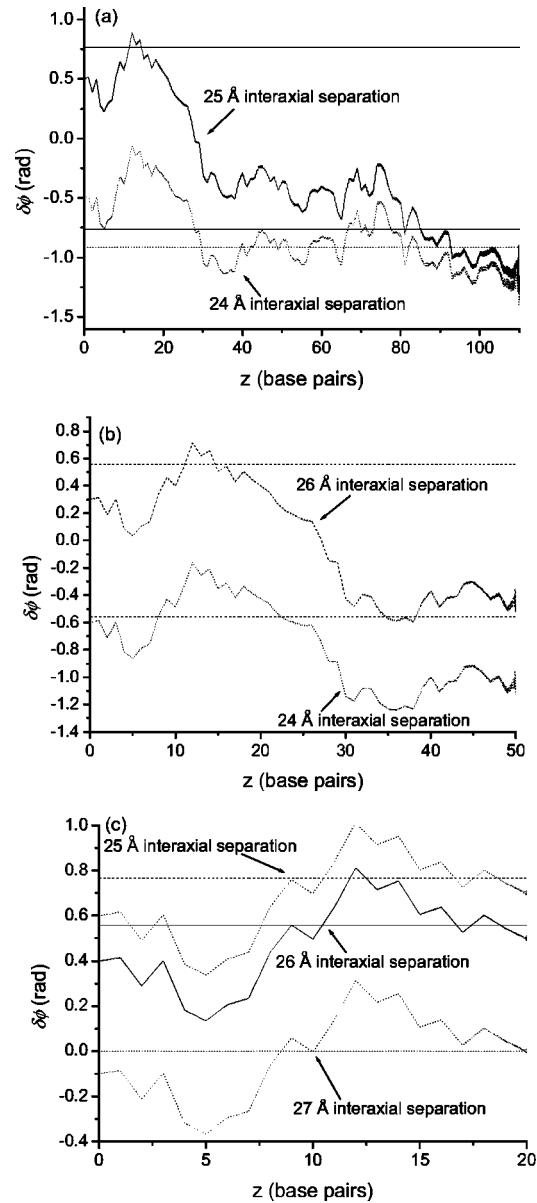


FIG. 10. Phase angle profiles for sequences of different lengths. For the 110 base pair duplexes (a), a first-order transition occurs at an interaxial separation between 24 and 25 Å. At a separation of 25 Å, the phase angle is shared between the positive and negative optimal angles (shown as horizontal solid lines), but at closer separations below the transition, the phase angle centers around only one of these optimal angles (shown as a horizontal dotted line). This is likewise seen in (b) for 50 base pair duplexes. At some point, it is not long or flexible enough to be shared between the optimal angles. In (c), a 20 base pair fragment cannot be shared between the \pm optimal angles: it “has no room” to accommodate a small kink and simply follows one of the optimal angles (shown as horizontal lines). Thus the transition returns to second order occurring very close to the point of frustration of the interaction potential for identical helices.

VII. CONCLUDING REMARKS

In this paper, we have presented numerical studies demonstrating the existence of strong nonlinear effects in the interaction of two DNA duplexes. These nonlinearities

manifest themselves in the considerable kink-like twist deformations caused by interaction of nonhomologous duplexes. These, in turn, may be reflected in homologous recombination as it pertains to primary recognition between homologous DNA pairs. Furthermore, the dramatic structural heterogeneities associated with the torsional kinks also may be important for interactions between DNA and proteins [53,54].

We are currently applying similar numerical techniques to assemblies of duplexes where more tractable experiments probing the signatures of nonlinearity may be performed. A complete investigation of these effects, including their thermodynamic properties, may engender a variety of consequences for many processes involving DNA and its packing.

The present approach was based on a continuum approximation where one torsional rigidity modulus was attributed to the whole molecule. Variation in the base pair text can, in principle, create a situation where there exist large differences of the torsional forces for different sections of the molecule. Such a situation will require a special treatment. Preliminary investigations of a more discrete model, in which such effects may be incorporated, have already demonstrated consistency with the continuum ones.

Having studied the effects of torsional deformations, we did not consider any additional charge restructuring in the pattern of adsorbed counterions which may accompany torsional adjustment. Such effects have been studied separately for torsionally rigid molecules [55]. Considering two processes simultaneously would be more appropriate in a fully atomistic approach of molecular dynamics which is also underway.

Further analytical studies are presently underway to reveal if there are any general laws in recognition and torsional

adjustment. Also, some experiments will soon be undertaken so that certain predictions of this model may be tested before further speculation about the possible biological implications of “love at first sight” between helical macromolecules.

ACKNOWLEDGMENTS

The expectations of the possible importance of the static kink-like effects emerged from joint work with Sergey Leikin and estimates made together. Some studies in the doctoral work of and discussions with Andrey Cherstvy have influenced this study. Richard Craster’s advice on the numerical procedures was critical at the early stages of this work. Support of EPSRC Grant No. 531068/01 and a Royal Society Wolfson Merit Research Award (A.A.K.) are gratefully acknowledged.

APPENDIX A: THE SOLUTION OF THE HOMOGENOUS EULER EQUATION

For infinitely long molecules with boundary conditions of zero phase angle derivatives at $\pm\infty$, the solutions of Eq. (2) can be compactly written in terms of the parameter $\gamma = 2a_2/a_1$.

(1) z -independent solutions:

$$\delta\phi = \begin{cases} \pm \arccos\left(\frac{1}{2\gamma}\right), & \gamma > 1/2, \\ 0, & \gamma < 1/2. \end{cases} \quad (\text{A1})$$

(2) Kink-soliton-like solutions:

$$\delta\phi(z) = \begin{cases} \pm 2 \arctan\left\{ \sqrt{\frac{2\gamma-1}{2\gamma+1}} \tanh\left[\frac{z-z_0}{2\lambda_t} \sqrt{\frac{4\gamma^2-1}{2\gamma}}\right] \right\}, & \gamma \geq 1/2, \\ \arccos\left\{ \frac{\sinh^2\left[\frac{\sqrt{1-2\gamma} \frac{z-z_0}{\lambda_t}}\right] - (1-2\gamma)}{\sinh^2\left[\frac{\sqrt{1-2\gamma} \frac{z-z_0}{\lambda_t}}\right] + (1-2\gamma)} \right\}, & \pm(z-z_0) < 0, \gamma \leq 1/2, \\ 2\pi - \arccos\left\{ \frac{\sinh^2\left[\frac{\sqrt{1-2\gamma} \frac{z-z_0}{\lambda_t}}\right] - (1-2\gamma)}{\sinh^2\left[\frac{\sqrt{1-2\gamma} \frac{z-z_0}{\lambda_t}}\right] + (1-2\gamma)} \right\}, & \pm(z-z_0) > 0, \gamma \leq 1/2. \end{cases} \quad (\text{A2})$$

In the particular case of $\gamma=0$ these are, correspondingly, the trivial solution $\delta\phi=0$ and the well known sine-Gordon kink $\delta\phi = 4 \arctan[\exp\{\pm(z-z_0)/\lambda_t\}]$.

The free energy needed to excite a soliton (in the absence of the random field) is obtained by substitution of these

solutions into Eq. (2). The energies for the solitons—the “small” one, at $\gamma > 1/2$, i.e., existing at short distances between the molecules, and the “large” one, at $\gamma < 1/2$, i.e., existing at long distances between the molecules—are given, respectively, by

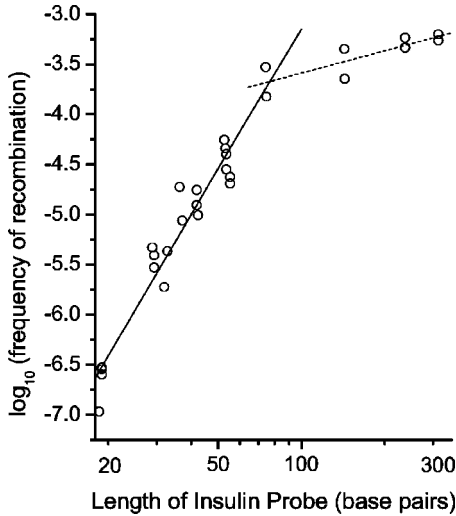


FIG. 11. Frequency of recombination as a function of length of homologous insulin DNA fragments reproduced from Ref. [17]. Each experimental point represents a single determination of recombination frequency from separate recombination experiments. Straight line fits were made for lengths from 20 to 74 base pairs (solid line) and for lengths from 74 to 313 base pairs (dotted line).

$$E^* = \sqrt{Ca_1} f(2\gamma),$$

$$f(x) = \begin{cases} \sqrt{2x} \left[\sqrt{1 - \frac{1}{x^2}} - \frac{\arccos(1/x)}{x} \right], & x > 1, \\ 2\sqrt{2} \left[\sqrt{1-x} + \frac{\arcsin \sqrt{x}}{\sqrt{x}} \right], & x < 1. \end{cases} \quad (\text{A3})$$

The lower line (large soliton) corresponds to a torsional rotation from 0 azimuthal angle to an azimuthal angle of 2π , whereas the upper line (small soliton) corresponds to a rotation between $\pm \arccos(1/2\gamma)$. In the region of existence of small solitons there is also a higher-order excitation, a rotation between $\pm \arccos(1/2\gamma)$ and $2\pi \mp \arccos(1/2\gamma)$, whose energy is given by

$$E^{**} = \sqrt{Ca_1} F(2\gamma),$$

$$F(x) = \sqrt{2x} \left[\sqrt{1 - \frac{1}{x^2}} + \frac{(\pi/2) + \arcsin(1/x)}{x} \right]. \quad (\text{A4})$$

At $\gamma=1/2$, E^{**} merges with the $x < 1$ branch of E^* . The energies for these different kinks are compared in Fig. 12. It shows that the large soliton kinks are large energy excitations of the system which would not likely be thermally activated over this interaxial separation range. However, small solitons have energies close to or even less than $k_B T$ (especially near the frustration point) and therefore must be considered viable phase angle solutions at finite temperatures.

APPENDIX B: FRENKEL-KONTOROVA LIMIT: $\delta\Omega = \text{const}$

When $\delta\Omega$ is constant rather than random, Eq. (1) excluding the second cosine term has the energy form of the famous Frenkel-Kontorova model [46]. The FK model was

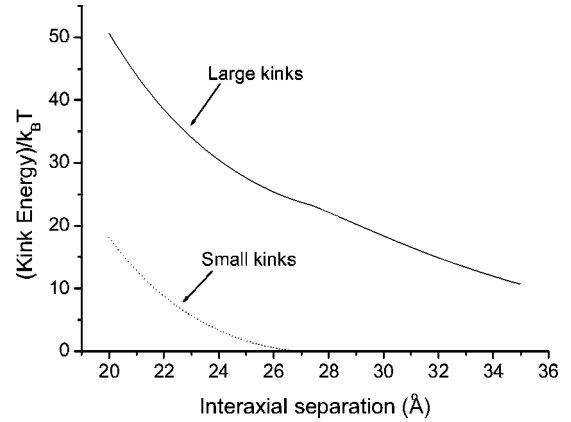


FIG. 12. The large and small kink energies for the free soliton solutions, Eqs. (A1) and (A2), as a function of interaxial separation between DNA molecules. The same electrostatic and torsional parameters used in Figs. 6–10 were also used here to generate these energies. Note that the energy of the small kink decays quickly to zero near the frustration point, which occurs at approximately 27 Å. The energy of the large kink remains quite large over this entire interaxial separation range.

originally suggested to describe a one-dimensional string of atoms, treated as a harmonic chain of a certain periodicity, adsorbed onto a substrate of another periodicity. The resulting structure of the chain depends entirely on the competition between the parameters that characterize the strength of attraction to the substrate, elasticity of the chain springs, and the ratio of the equilibrium period of the free chain to the period of the substrate potential. If the attraction is strong and the chain is soft it will adjust to the periodicity of the substrate. If the chain is rigid and the periods are incommensurate, the chain will be in the so-called floating phase, incommensurate with the substrate. In intermediate cases there is a complicated phase diagram on the plane of parameters characterizing the ratio of the strength of the potential to the rigidity of the springs and the ratio of the periodicity of the springs to the substrate period. The solutions will contain the periodicity domains separated by the defect regions—domain walls—which are narrow if the interaction is strong or wide if it is weak. This model appears to be important in different areas of physics, viz. the theory of dislocations, commensurate-incommensurate phase transitions, domain walls in magnetically ordered structures, etc. Solutions of this model are well studied.

We can apply a similar analysis to the model of interacting DNA if we assume that the preferred twist angles between DNA duplexes are offset by the same amount $\delta\Omega = \eta$ at each base pair step. This leads to a phase accumulation term $\Psi(z) = \eta z/h$, that simply increases linearly along the juxtaposition length. For perfectly rigid duplexes where the torsional force constant is infinite, the phase angle follows this accumulation [see Fig. 13(a)]. This case, in terms of the FK model, corresponds to perfect incommensurability where there is no correlation between the periodicity response of the phase, which is locked in at η , and the 2π periodicity of the electrostatic interaction potential. For extremely soft molecules, i.e., when the torsional force constant C is quite small, the phase angle solution is almost zero everywhere corresponding to nearly perfect commensurabil-

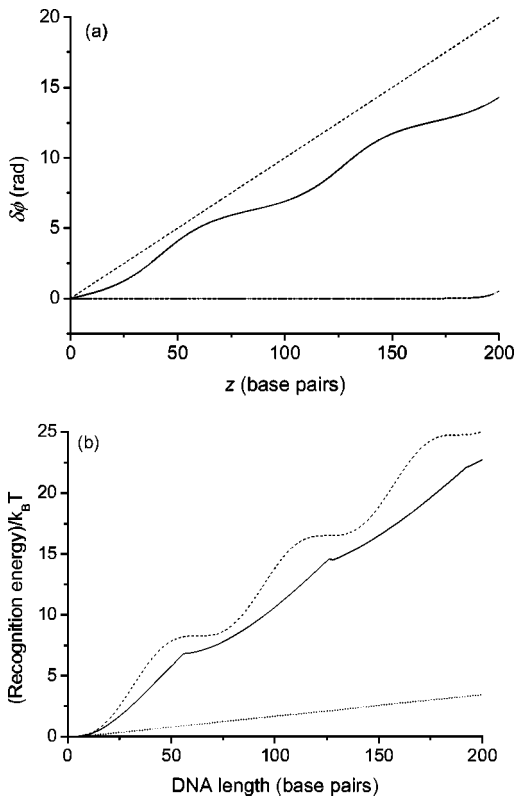


FIG. 13. The phase angle (a) and the recognition energy (b) in the Frenkel-Kontorova limit. The dotted line corresponds to extremely soft molecules, $C=1.0 \times 10^{-20}$ ergs cm, and the dashed line to perfectly rigid molecules $C=\infty$. For an intermediate value $C=1.0 \times 10^{-19}$ ergs cm (the solid curve), solitonlike kinks emerge in the phase angle demonstrating the interplay between the torsional forces and the 2π periodic electrostatic potential. The electrostatic parameter used here was $a_1=16.0 \times 10^{-8}$ ergs/cm. In these calculations the phase angle was fixed to zero at the left side.

ity. At intermediate values of C , soliton-like modes appear (as they did in the case of random $\delta\Omega$), favoring the 2π periodicity of the electrostatic potential so that along the length of juxtaposition, there are regions of greater “commensurability” of the resulting phase angle. But the accumulation of mismatch is much faster now and thus must be relaxed by a larger number of solitons.

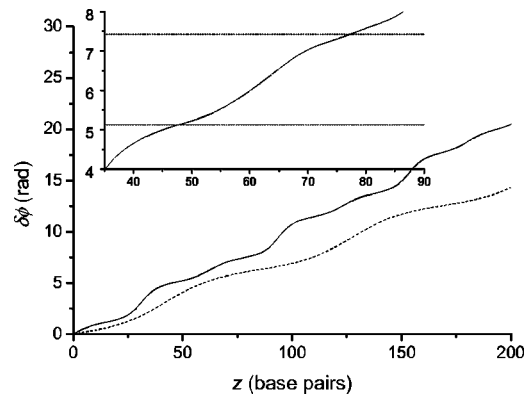


FIG. 14. The effect of the frustration of the interaction potential in the Frenkel-Kontorova limit. Adding the frustration term results in the solid curve for the phase angle. The 2π soliton kink (the dashed curve) of Fig. 13(a) is also shown here for reference. As shown in the inset, the flatter regions are now centered about the \pm optimal angles of Eq. (4) (shown as the horizontal dashed flat lines) for duplexes within the region of frustration. The parameters for the frustrated phase angle solution are $C=0.3 \times 10^{-19}$ ergs cm, $a_1=16.0 \times 10^{-8}$ ergs/cm, and $a_2=10.0 \times 10^{-8}$ ergs/cm. The boundary condition is the same as in Fig. 13.

This effect translates into the peculiar curve of the recognition energy as a function of juxtaposition length, or the length of homology, Fig. 13(b). For the case of rigid duplexes, this curve is very different than for random $\delta\Omega$ (Fig. 2 of Ref. [10]). For the intermediate case, the plateau structure seen in the recognition energy of the rigid case is partially relaxed. As the molecules become even softer, the recognition energy becomes linear in the juxtaposition length.

Similar effects in the phase angle are observed when the second cosine, the “frustration,” term is included (Fig. 14). Going beyond the standard Frenkel-Kontorova limit, the inclusion of frustration leads to distortions of the 2π kinks depending on the relative strength of the frustration term to the first cosine term. As in our model where $\delta\Omega$ is random, this distortion from the usual 2π kink-soliton modes appears simply as smaller kinks between the \pm optimal angles. The locations of greater commensurability, where the phase angle curve is the flattest, are now centered about these optimal angles.

-
- [1] W. M. Gelbart, R. F. Bruinsma, P. A. Pincus, and V. A. Parsegian, *Phys. Today* **53**, 38 (2000).
 [2] Y. Levin, *Rep. Prog. Phys.* **65**, 1157 (2002).
 [3] D. M. Frank-Kamenetskii, V. V. Anshelevich, and A. V. Lukashin, *Sov. Phys. Usp.* **30**, 317 (1987).
 [4] A. A. Kornyshev and S. Leikin, *J. Chem. Phys.* **107**, 3656 (1997); **108**, 7035(E) (1998).
 [5] A. A. Kornyshev and S. Leikin, *Phys. Rev. Lett.* **82**, 4138 (1999).
 [6] H. H. Strey, J. Wang, R. Podgornik, A. Rupprecht, L. Yu, V. A. Parsegian, and E. B. Sirota, *Phys. Rev. Lett.* **84**, 3105 (2000).
 [7] V. Lorman, R. Podgornik, and B. Žekš, *Phys. Rev. Lett.* **87**, 218101 (2001).
 [8] H. M. Harreis, A. A. Kornyshev, C. N. Likos, H. Löwen, and G. Sutmann, *Phys. Rev. Lett.* **89**, 018303 (2002).
 [9] H. M. Harreis, C. N. Likos, and H. Löwen, *Biophys. J.* **84**, 3607 (2003).
 [10] A. A. Kornyshev and S. Leikin, *Phys. Rev. Lett.* **86**, 3666 (2001).
 [11] R. R. Sinden, *DNA Structure and Function* (Academic Press, San Diego, 1994).
 [12] S. Neidle, *DNA Structure and Recognition* (IRL Press at Oxford University Press, Oxford, 1994).
 [13] A. A. Gorin, V. B. Zhurkin, and W. K. Olson, *J. Mol. Biol.*

- 247**, 34 (1995).
- [14] W. Kabsch, C. Sander, and E. N. Trifonov, *Nucleic Acids Res.* **10**, 1097 (1982).
- [15] W. K. Olson, A. A. Gorin, X.-J. Lu, L. M. Hock, and V. B. Zhurkin, *Proc. Natl. Acad. Sci. U.S.A.* **95**, 11 163 (1998).
- [16] B. S. Singer, L. Gold, P. Gauss, and D. H. Doherty, *Cell* **31**, 25 (1982).
- [17] V. M. Watt, C. J. Ingles, M. S. Urdea, and W. J. Rutter, *Proc. Natl. Acad. Sci. U.S.A.* **82**, 4768 (1985).
- [18] S. Subramani and P. Berg, *Mol. Cell. Biol.* **3**, 1040 (1983).
- [19] J. Rubnitz and S. Subramani, *Mol. Cell. Biol.* **4**, 2253 (1984).
- [20] C. Deng and M. R. Cappechi, *Mol. Cell. Biol.* **12**, 3365 (1992).
- [21] S. Jink-Robertson, M. Michelitch, and S. Ramcharan, *Mol. Cell. Biol.* **13**, 3937 (1993).
- [22] B. Lewin, *Genes VI* (Oxford University, Oxford, 1997).
- [23] B. M. Weiner and N. Kleckner, *Cell* **77**, 977 (1994).
- [24] S. M. Burges, N. Kleckner, and M. Weiner, *Genes Dev.* **13**, 1627 (1999).
- [25] Y. Fujitani and I. Kobayashi, *Phys. Rev. E* **52**, 6607 (1995).
- [26] Y. Fujitani, K. Yamamoto, and I. Kobayashi, *Genetics* **140**, 797 (1995).
- [27] *DNA need not unzip*, *Phys. Rev. Focus* (<http://focus.aps.org/story/v7/st19.html>).
- [28] A. G. Cherstvy, A. A. Kornyshev, and S. Leikin, *J. Phys. Chem.* (to be published).
- [29] S. B. Zimmerman and B. H. Pfeiffer, *Proc. Natl. Acad. Sci. U.S.A.* **76**, 2703 (1979).
- [30] J. C. Wang, *Proc. Natl. Acad. Sci. U.S.A.* **76**, 200 (1979).
- [31] D. Rhodes and A. Klug, *Nature (London)* **286**, 573 (1980).
- [32] R. Langridge, H. R. Wilson, C. W. Hooper, M. H. F. Wilkins, and L. D. Hamilton, *J. Mol. Biol.* **2**, 19 (1960).
- [33] W. Fuller, M. H. F. Wilkins, H. R. Wilson, and L. D. Hamilton, *J. Mol. Biol.* **12**, 60 (1965).
- [34] A. A. Kornyshev and S. Leikin, *Biophys. J.* **75**, 2513 (1998).
- [35] A. A. Kornyshev and S. Leikin, *Proc. Natl. Acad. Sci. U.S.A.* **95**, 13579 (1998).
- [36] In this paper we explore exclusively the effect of the torsional degrees of freedom of the molecules, ignoring the effects of bending. The bending persistence length is believed to be of the same order of magnitude as the torsional one. However, in order to relax the mismatch caused by the twist angle distortions, torsional adaptation should be the measure of choice, unless the chiral twist effects [A. A. Kornyshev and S. Leikin, *Phys. Rev. Lett.* **84**, 2537 (2000); A. A. Kornyshev, S. Leikin, and S. V. Malinin, *Eur. Phys. J. E* **7**, 83 (2002)] are to cause supercoiling. Charges on the polyelectrolyte molecule are known to affect the rigidity moduli of DNA. For instance in the Odijk-Skolnick-Fixman theory [T. J. Odijk, *Polym. Sci. U.S.S.R.* **15**, 477 (1977); J. Skolnick and M. Fixman, *Macromolecules* **10**, 944 (1977)] the persistence length of a helical polyelectrolyte depends on the net charge of the molecule. The latter causes screened intrastrand electrostatic forces that make the molecule more rigid to bending. The torsional adaptation driven by the electrostatic interaction between juxtaposing DNA duplexes, belongs to the same class of phenomena. However, as considered in the present work, the electrostatic interaction between the duplexes provokes torsional relaxation, but within the harmonic description of the local torsional deformations their rigidity modulus stays unchanged.
- [37] D. M. Crothers, J. Drak, J. D. Kahn, and S. D. Levene, in *Methods in Enzymology*, edited by D. M. J. Lilley and J. E. Dahlberg (Academic Press, San Diego, 1992), Vol. 212 B, p. 3, and references therein.
- [38] D. Shore and R. Baldwin, *J. Mol. Biol.* **170**, 957 (1983).
- [39] M. D. Frank-Kamenetskii, A. V. Lukashin, V. V. Anshelevich, and A. V. Vologodskii, *J. Biomol. Struct. Dyn.* **2**, 1005 (1985).
- [40] H. S. Strogatz, *Nonlinear Dynamics and Chaos: With Applications to Physics, Biology, Chemistry and Engineering* (Addison-Wesley, Reading, MA, 1994).
- [41] H. Reininger and F. Schwable, *Z. Phys. B: Condens. Matter* **52**, 151 (1983).
- [42] J. P. Boyd, *Chebyshev and Fourier Spectral Methods* (Dover Publications, Mineola, NY, 2000).
- [43] G. W. Wei, D. S. Zhang, D. J. Kouri, and D. K. Hoffman, *Phys. Rev. Lett.* **79**, 775 (1997).
- [44] D. J. Kouri, D. S. Zhang, G. W. Wei, T. Konshak, and D. K. Hoffman, *Phys. Rev. E* **59**, 1274 (1999).
- [45] This statement should not be taken literally but is intended to give a flavor of what is the main driving force for relaxation.
- [46] P. M. Chaikin and T. C. Lubensky, *Principles of Condensed Matter Physics* (Cambridge University Press, Cambridge, 2000), Chap. 10.
- [47] Such sequences will have different torsional elastic constants. Taking this into account will eliminate the exact correspondence to the Frenkel-Kontorova problem. In Appendix B differences in C 's are not implied.
- [48] A. C. Scott, *Mol. Cell. Biol.* **3**, 5 (1985).
- [49] G. Gaeta, C. Reiss, M. Peyrard, and T. Dauxis, *Riv. Nuovo Cimento* **17**, 1 (1994).
- [50] *Nonlinear Excitations in Biomolecules*, edited by M. Peyrard (Springer, Berlin, 1995).
- [51] L. V. Yakushevich, *Nonlinear Physics of DNA* (Wiley, Chichester, 1998).
- [52] P. Shen and H. V. Huang, *Genetics* **112**, 441 (1986), and the references cited therein.
- [53] Z. Otwinowski, R. W. Schevit, R.-G. Zhang, C. L. Lawson, A. Joachimiak, R. Q. Marmorstein, B. F. Luisi, and P. B. Sigler, *Nature (London)* **335**, 321 (1998).
- [54] C. R. Calladine and H. R. Drew, in *Molecular Structure and Life*, edited by Y. Kyogoku and Y. Nishimura (CRC Press, Boca Raton, FL, 1992), pp. 43–55.
- [55] A. G. Cherstvy, A. A. Kornyshev, and S. Leikin, *J. Phys. Chem. B* **106**, 13 362 (2002).